Supplementary Information

Cooling and shading corals: *in-situ* mitigation of bleaching through engineered refuges

Claire Boitel[1]*, Océane Moeino[1], Caroline Bonpain[1], Camille Gache[1], Hugo Bischoff[1], Emilie Boissin[1], Jade Noailly[1], Serge Planes[2] & Laetitia Hédouin[1]

Supplementary results

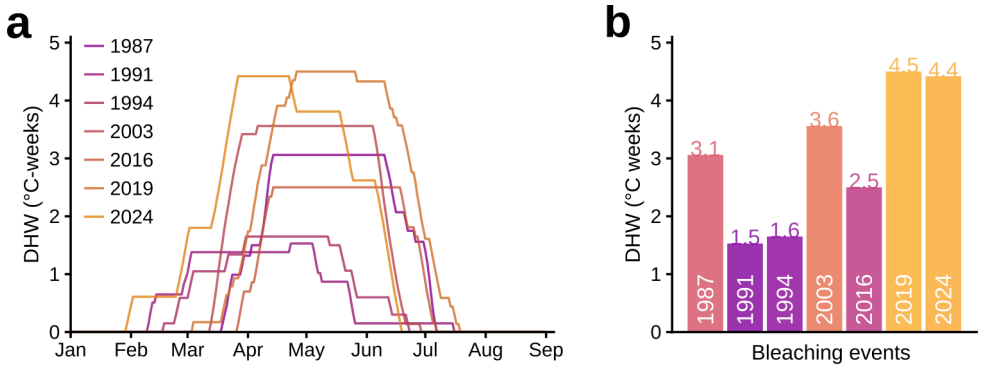

Supplementary Figure 1. Severity of the 2024 marine heatwave relative to previous thermal anomalies (1985-2023). (a) Temporal evolution of accumulated thermal stress (Degree Heating Weeks, DHW) from the NOAA Coral Reef Watch 5-km satellite-derived SST product. (b) Cumulative summer DHW across bleaching years between 1985 and 2024.

Supplementary Table 1. Pairwise post-hoc Tukey t-tests of differences in estimated marginal means of daily temperaturemeans and daily thermal range between control and shaded nurseries, and cooled nurseries while interventions were deployed

Contrast	estimate	SE	df	z.ratio	p-value	
Mean daily temperature						
Control and shade – Cooling	0.711	0.004	Inf	195.75	< 0.0001	***
Daily range						
Control and shade – Cooling	-0.353	0.038	134	-9.36	< 0.0001	***

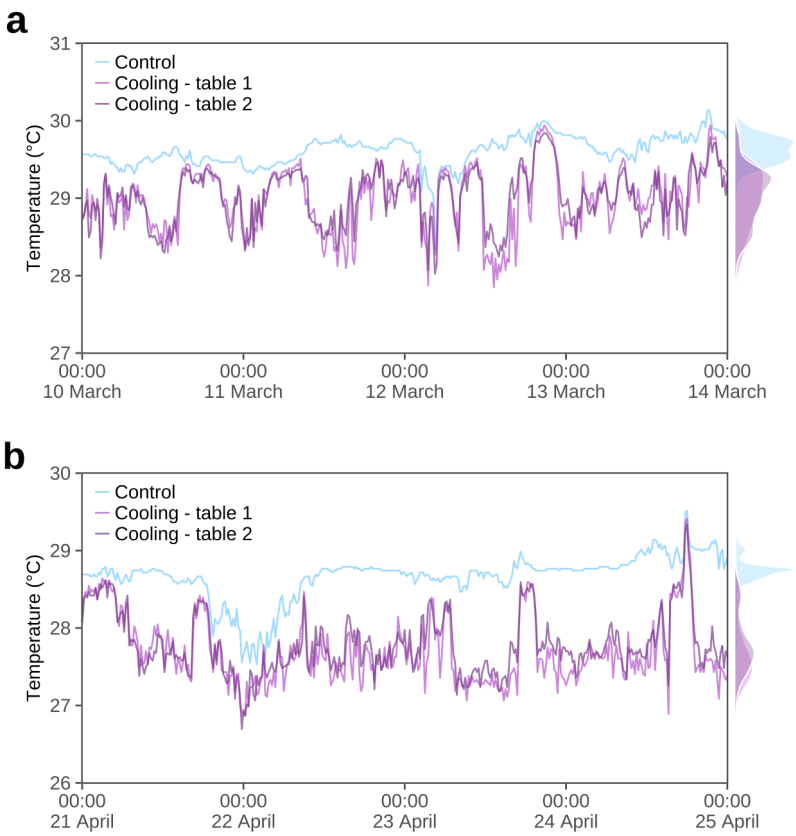

Supplementary Figure 2. Dynamics of cooling during the 2024 marine heatwave. (a) Four-day temperature records at the beginning of the heatwave (mid-March) and (b) around peak thermal stress (end of April). Control and shaded nurseries are shown in blue; cooled tables (1 and 2) in violet shades. Kernel density plots (right panels) summarize temperature distributions over each period, illustrating temporal variability in cooling performance, depending on currents.

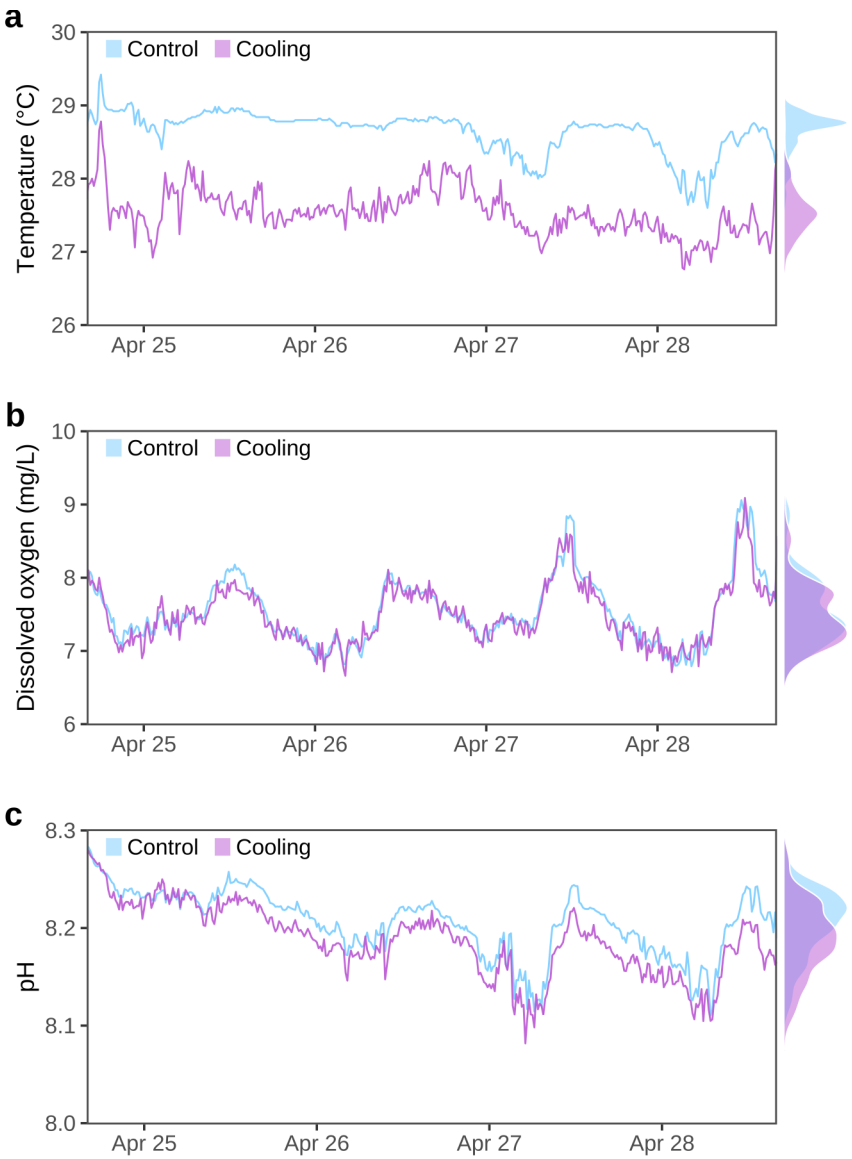

Supplementary Figure 3. Water chemistry responses to deep-water diffusion, depended on (a) cooling intensity. (b) Dissolved oxygen concentrations and (c) pH variation across treatments were measured during t1 (24-28 April) by deploying respectively HOBO U26-001 and HOBO MX pH loggers at fragment height; sensors were positioned centrally within cooled tables for the cooling treatment.

Supplementary Table 2. Pairwise post-hoc Tukey t-tests of differences in estimated marginal means of nutritive salts concentrations (from top to bottom: ammonium, nitrites, nitrates, phosphates and silicates) between control and cooled tables. Dissolved inorganic nitrogen (DIN) is the computed by summing concentrations of ammonium, nitrite and nitrate. Contrasts are ratios of Control / Cooling emmeans.

Nutrient	**ratio**	**SE**	**df**	**z.ratio**	**p-value**	
NH_4^+	0.642	0.147	Inf	-1.933	0.0532	
NO_2^-	1.667	0.364	Inf	2.337	0.0194	**
NO_3^-	0.074	0.016	Inf	-11.913	< 0.0001	***
PO_4^{3-}	0.924	0.202	Inf	-0.360	0.7189	
$SI(OH)_4$	0.282	0.0620	Inf	-5.790	< 0.0001	***
Dissolved inorganic nitrogen (DIN)	0.159	0.026	Inf	-11.285	< 0.0001	***

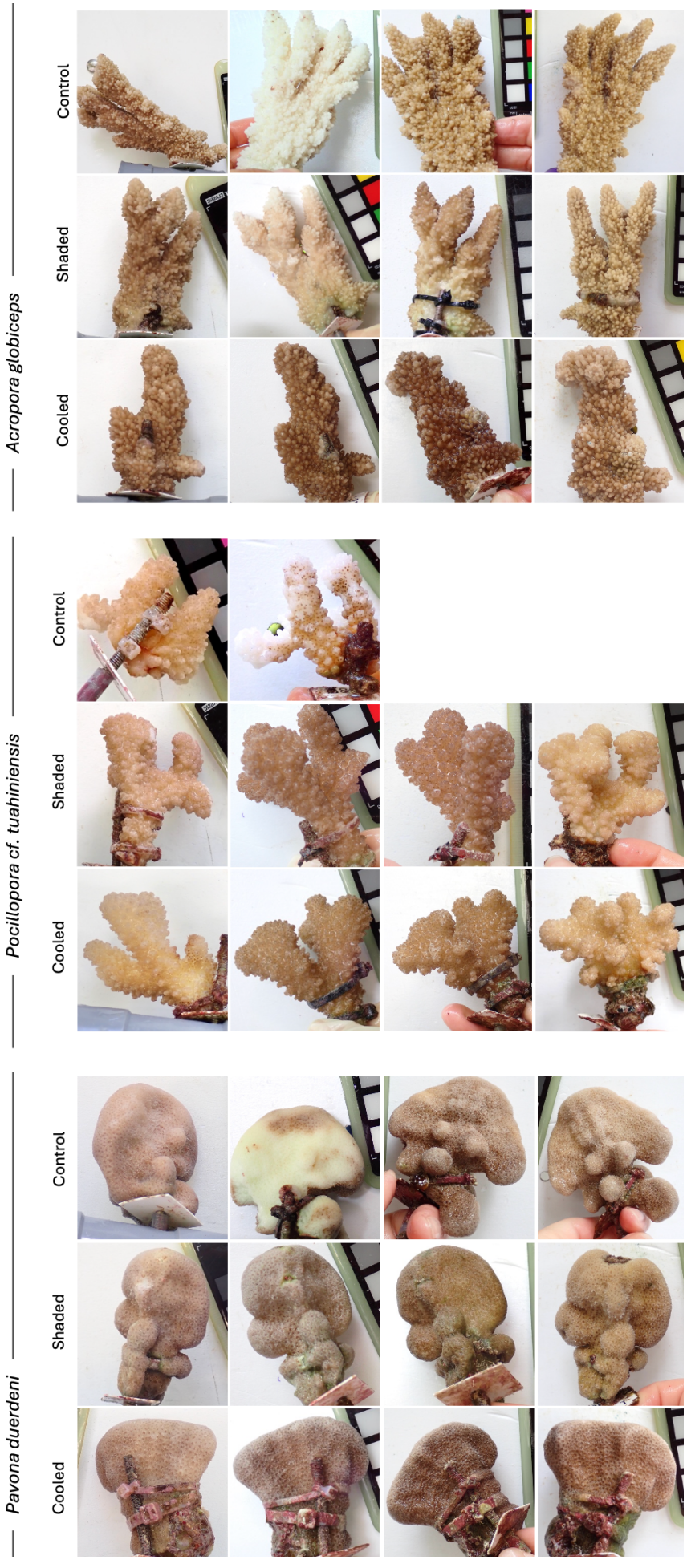

◄ Supplementary Figure 4. Temporal pigmentation dynamics in *Acropora globiceps, Pocillopora cf. tuahiniensis,* and *Pavona duerdeni* (from top to bottom) across treatments. Representative fragments illustrating treatment-specific bleaching responses were selected (same fragment tracked over time). Photographs were taken before heatwave onset and deployment of interventions (February, t0), at peak heat stress (April, t1), prior to intervention cessation (July, t2), and four months post-intervention (November, t3). Note how in April, *P. cf. tuahiniensis* exhibited partial bleaching on the upper fragment surface while retaining stronger pigmentation on the underside, relative to pre-bleaching.

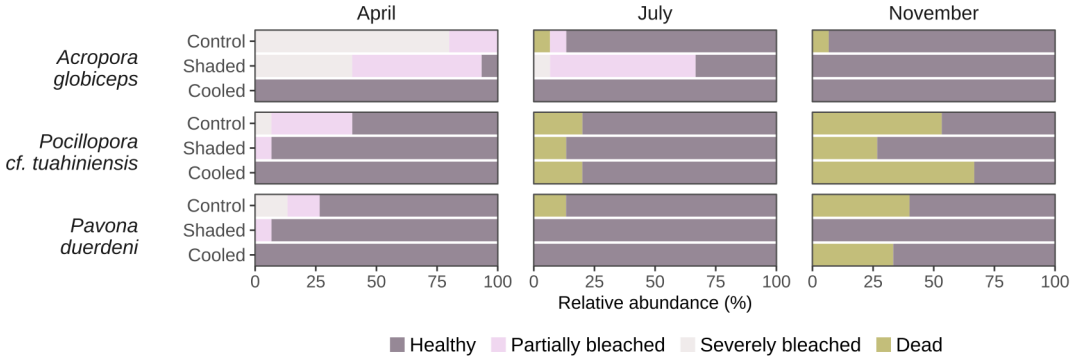

Supplementary Figure 5. Fragment health trajectories throughout the experiment in April (peak marine heatwave), in July (when interventions were ceased) and in November, during recovery, 4 months post-intervention. Fragments were considered partially bleached when 10-70% of their surface was depigmented, severely bleached when >70% was depigmented, or dead if no live tissue remained.

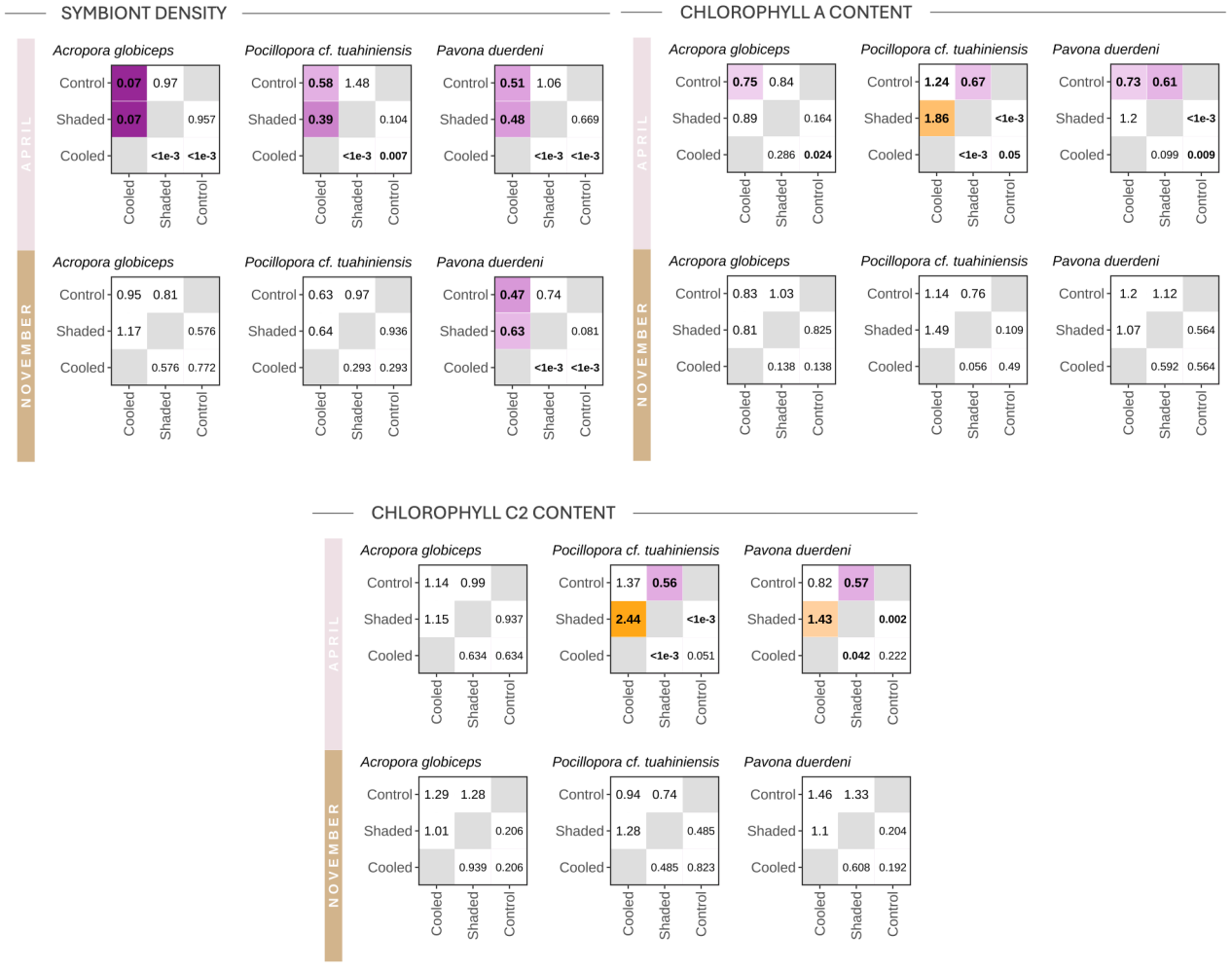

Supplementary Figure 6. Pairwise post-hoc contrasts among treatments for symbiont density and chlorophyll content. Benjamini-Hochberg-adjusted pairwise comparisons are shown for symbiont density, chlorophyll a per symbiont, and chlorophyll c2 per symbiont at peak heat stress (April) and during recovery (November, 4 months post-intervention). Upper-left triangles display ratios of estimated marginal means (emmeans; Y-axis / X-axis). Lower-right triangles show corresponding adjusted contrast p-values. Significant differences are indicated in bold and colored according to effect direction and magnitude (ratios > 1 in shades of orange; ratios < 1 in shades of purple).

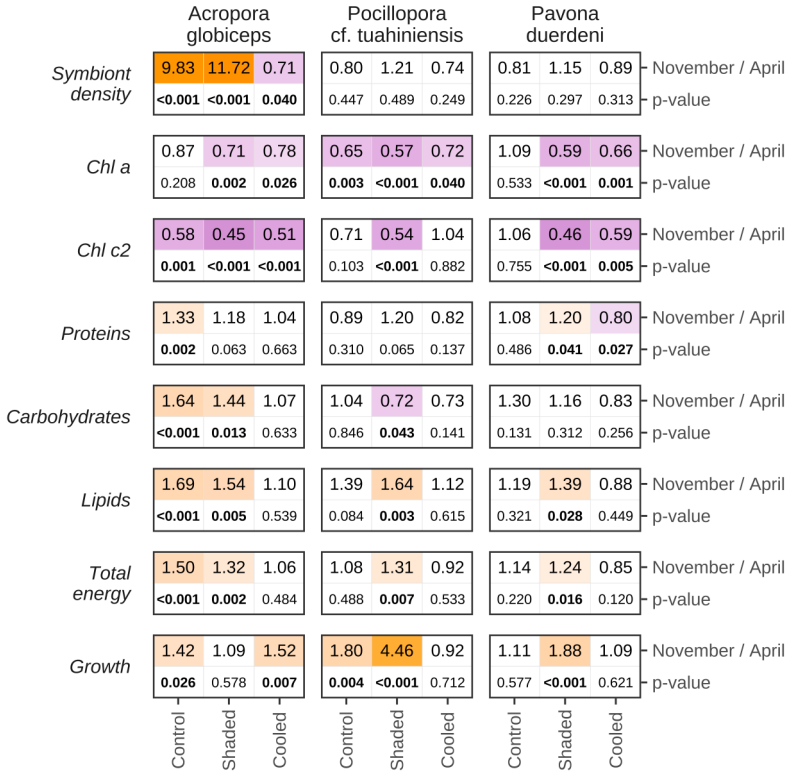

Supplementary Figure 7. Pairwise post-hoc contrasts between April and November across physiological variables. Benjamini-Hochberg-adjusted comparisons are shown for symbiont density, chlorophyll content, proteins, lipids, carbohydrates, total energy, and growth. The first row displays ratios of estimated marginal means (emmeans; November / April), and the second row shows the corresponding adjusted contrast p-values. Significant differences are colored according to effect direction and magnitude (ratios > 1 in shades of orange; ratios < 1 in shades of purple).

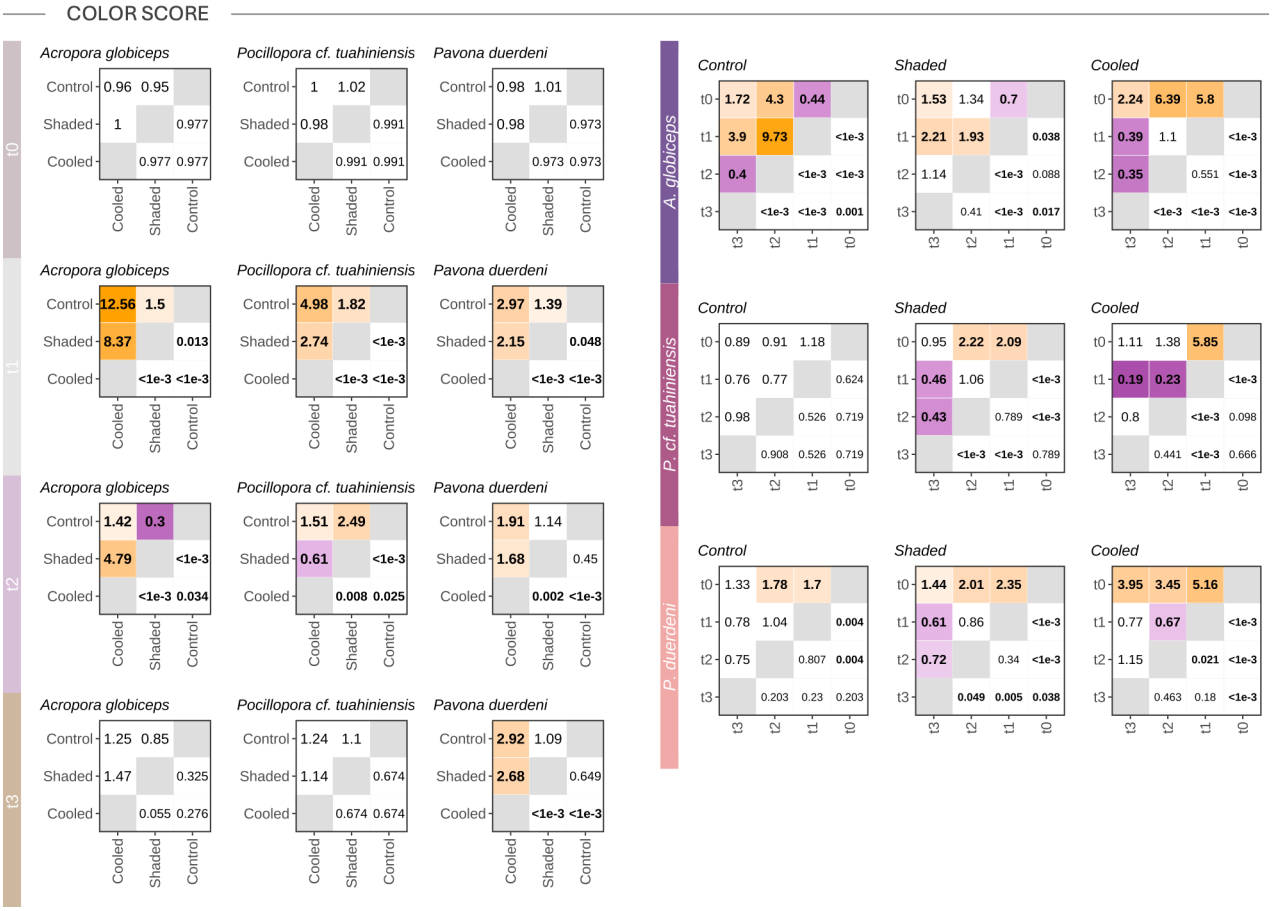

Supplementary Figure 8. Benjamini-Hochberg-adjusted pairwise post-hoc contrasts of color score across treatments and timepoints. Left panels show comparisons among treatments over time; right panels show comparisons among timepoints within each treatment. A higher color score indicates greater paling. Upper-left triangles display ratios of estimated marginal means (emmeans; Y-axis / X-axis). Lower-right triangles show corresponding adjusted contrast p-values. Significant differences are indicated in bold and colored according to effect direction and magnitude (ratios > 1 in shades of orange; ratios < 1 in shades of purple).

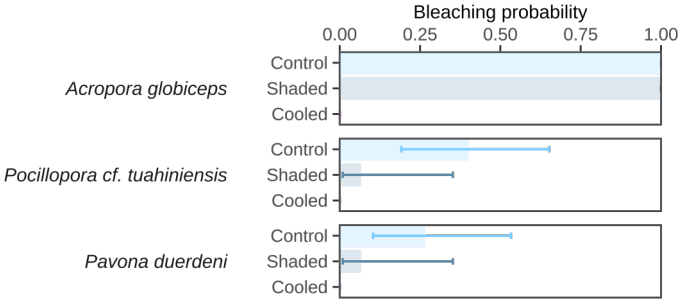

Supplementary Figure 9. Predicted probability of bleaching across treatments. Bleaching was defined as the occurrence of either partial or severe bleaching (i.e. exceeding physiological bleaching thresholds). Bars represent predicted probabilities from a binomial model and error bars indicate 95% confidence intervals.

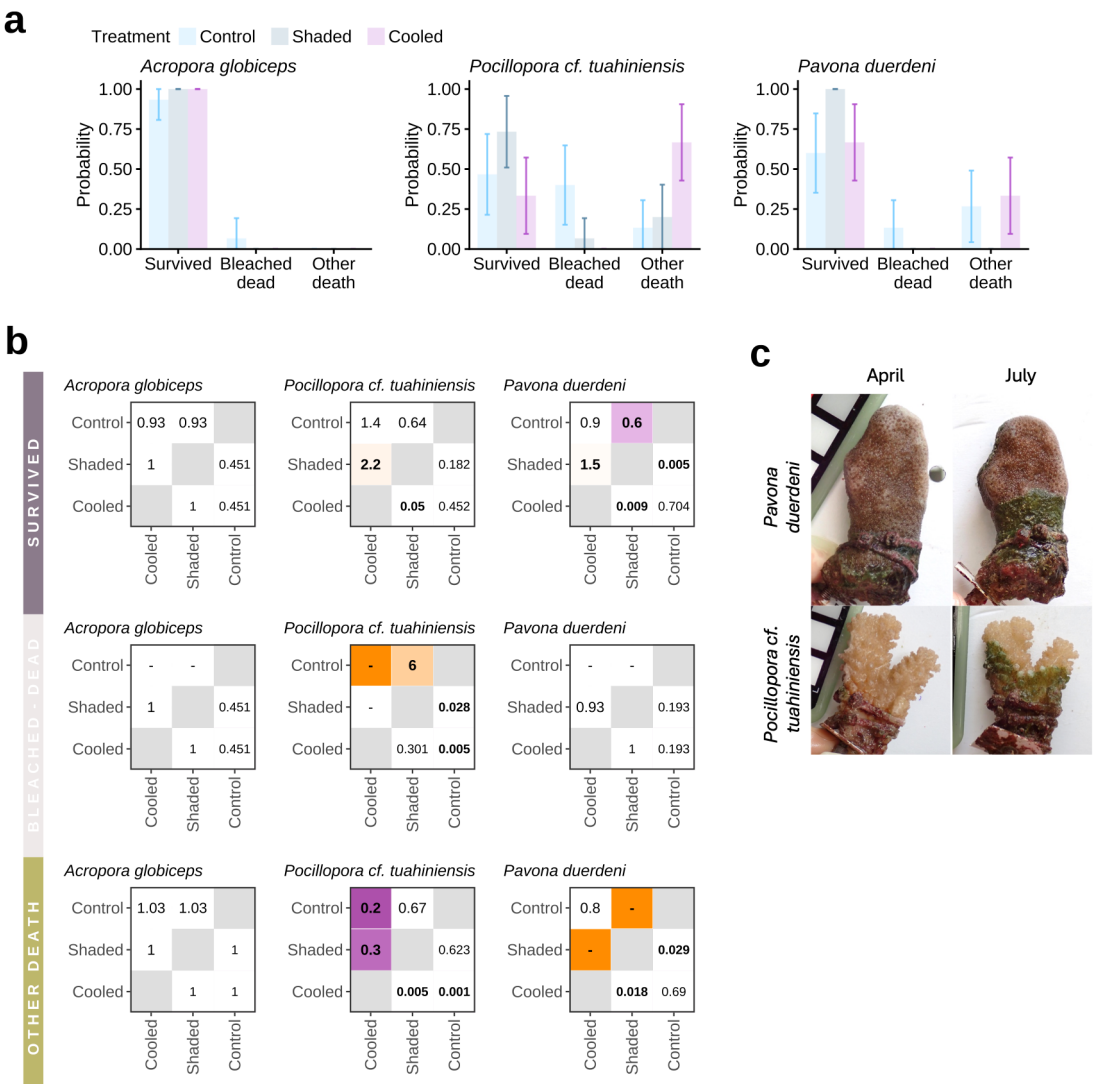

Supplementary Figure 10. Survival outcomes under the different treatments.
(a) Predicted probabilities of survival, bleaching-induced mortality, and non-bleaching mortality. Bars represent probabilities derived from a multinomial model and error bars indicate 95% confidence intervals. (b) Benjamini-Hochberg-adjusted pairwise post-hoc contrasts among treatments for each outcome category. Upper-left triangles display ratios of estimated marginal means (emmeans; Y-axis / X-axis). Lower-right triangles show corresponding adjusted contrast p-values. Significant differences are indicated in bold and colored according to effect direction and magnitude (ratios > 1 in shades of orange; ratios < 1 in shades of purple). (c) Representative photographs showing algal turf development on cooled fragments of *Pavona duerdeni* and *Pocillopora cf. tuahiniensis* classified as non-bleaching mortality ("other death") in November. Fragments were not visibly colonized at peak heat stress (April), whereas by July algal turf had expanded to cover at least half of the fragment surface.

Supplementary Figure 11. Pairwise post-hoc contrasts among treatments for energetic reserves. Benjamini-Hochberg-adjusted pairwise comparisons are shown for protein, lipid, carbohydrate content, and total energy (sum of the three macromolecule pools) at peak heat stress (April) and during recovery (November, 4 months post-intervention). Upper-left triangles display ratios of estimated marginal means (emmeans; Y-axis / X-axis). Lower-right triangles show corresponding adjusted contrast p-values. Significant differences are indicated in bold and colored according to effect direction and magnitude (ratios > 1 in shades of orange; ratios < 1 in shades of purple).

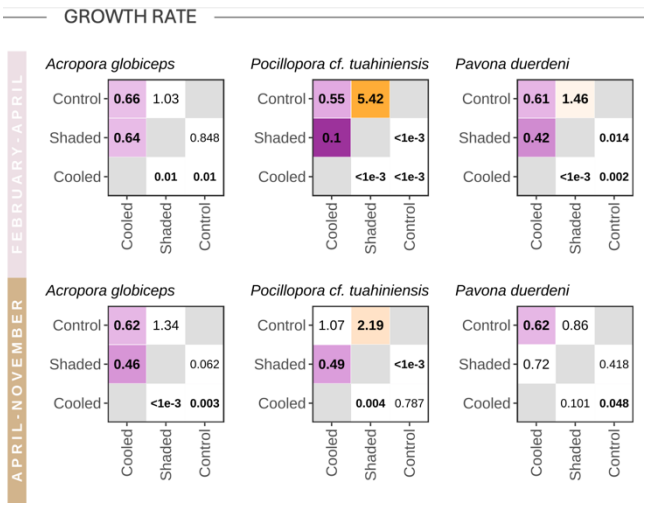

Supplementary Figure 12. Benjamini-Hochberg-adjusted pairwise contrasts among treatment for growth at peak heat stress (February-April) and during recovery (April-November, 4 months post-intervention). Upper-left triangles display ratios of estimated marginal means (emmeans; Y-axis / X-axis). Lower-right triangles show corresponding adjusted contrast p-values. Significant differences are indicated in

bold and colored according to effect direction and magnitude (ratios > 1 in shades of orange; ratios < 1 in shades of purple).

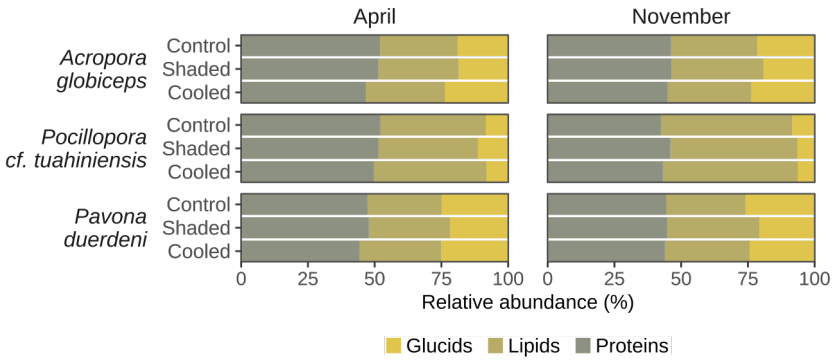

Supplementary Figure 13. Relative composition of total energetic reserves at peak heat stress and during recovery. Relative contributions of proteins, lipids, and carbohydrates to total energy are shown at peak heat stress (April) and four months post-intervention (November). The proportional contribution of each energetic compartment remained relatively stable over time within species and showed limited variation among treatments.

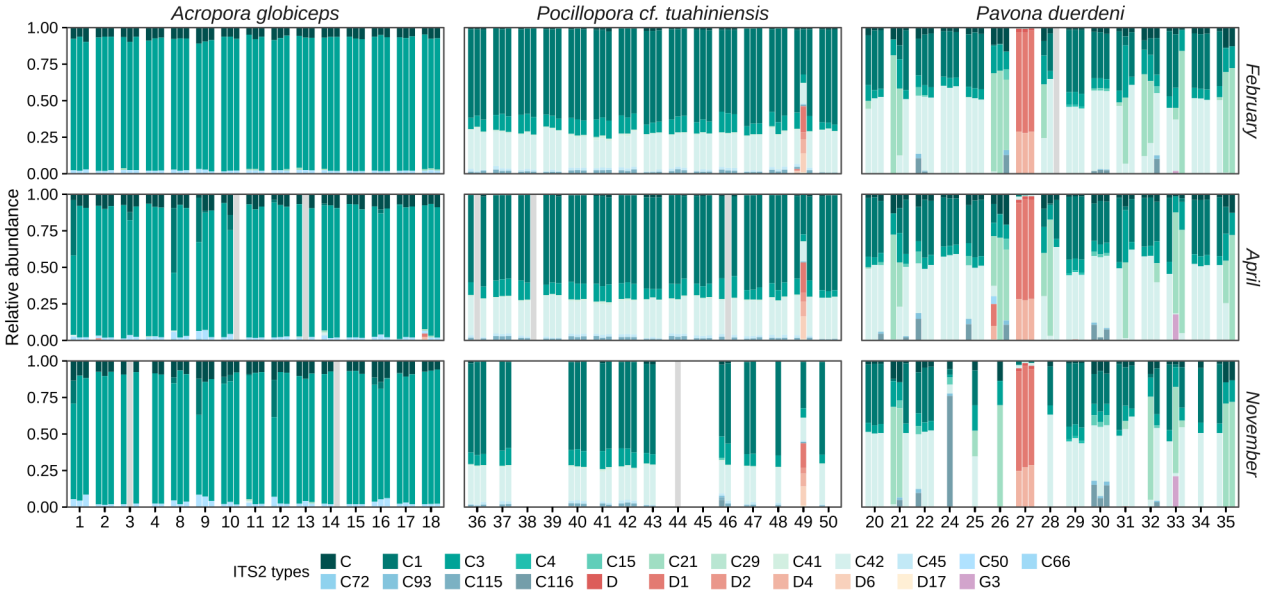

Supplementary Figure 14. Temporal evolution of *Symbiodiniaceae* communities within individual coral fragments across treatments as the relative abundance of the most abundant (> 0.01%) ITS2 subtypes. Each vertical bar represents a single fragment at a given timepoint: February (pre-intervention), April (peak marine heatwave), and November (4 months post-intervention, recovery phase). Grey bars corresponds to samples with unsuccessful sequencing. For each genotype within each species, three adjacent bars correspond to control, shaded, and cooled treatments (left to right). ITS2 subtypes were summarized to their major subtype to facilitate visualization (e.g. C3a and C3b grouped as C3). Due to the extensive ITS2 diversity catalogued in the SymPortal database, not all sequences are assigned names; unnamed *Cladocopium* and *Durusdinium* sequences (e.g. 25173_C) were therefore aggregated “C” and “D” types, respectively for visual representation.

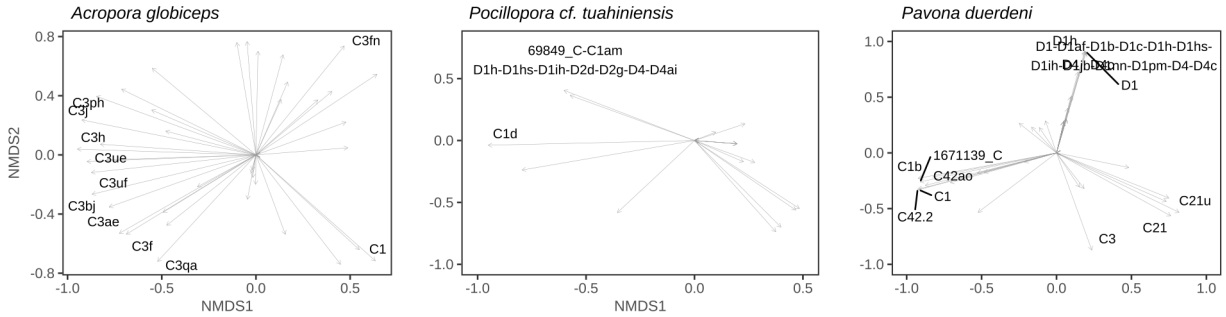

Supplementary Figure 15. Intragenomic variants (DIVs) associated with Symbiodiniaceae community shifts over time and across treatments. Displayed are sequence variants showing significant correlations with temporal and treatment-driven changes in *Symbiodiniaceae* community composition ($p < 0.05$). Only variants explaining more than 75% of the variance ($R^2 > 0.75$) are shown.

Supplementary Table 3. PERMANOVA results for dominant ITS2 profiles (with relative abundance > 0.01%).

Variable	Df	SumOfSqs	R^2	F	p	
Species	2	70,540	0,482	172,67	0,0001	***
Timepoint	2	0,664	0,005	1,62	0,0139	**
Treatment	2	0,917	0,006	2,25	0,0006	***
Species:Timepoint	4	1,183	0,008	1,45	0,0166	*
Species:Treatment	4	1,651	0,011	2,02	0,0006	***
Timepoint:Treatment	4	1,049	0,007	1,28	0,0164	*
Species:Timepoint:Treatment	8	1,955	0,013	1,20	0,0119	*
Residual	335	68,428	0,467			
Total	361	146,388	1			

Supplementary Table 4. Pairwise PERMANOVA results for dominant ITS2 profiles of *Acropora globiceps*.

Timepoint1	Timepoint2	Treatment1	Treatment2	R^2	F	p	
t0	t0	Control	Shaded	0,07134	2,1508	0,259	
		Control	Cooled	0,00001	0,0002	0,896	
		Shaded	Cooled	0,07135	2,1512	0,273	
t1	t1	Control	Shaded	0,08548	2,5237	0,1	
		Control	Cooled	0,23750	8,4101	0,002	**
		Shaded	Cooled	0,16656	5,1960	0,018	*
t3	t3	Control	Shaded	0,10996	3,2123	0,041	*
		Control	Cooled	0,17156	5,3843	0,018	*
		Shaded	Cooled	0,01639	0,4333	0,676	
t0	t1	Control	Control	0,12535	4,0127	0,018	*
t0	t3			0,21593	7,4358	0,037	*
t1	t3			0,08684	2,5677	0,077	

t0	t1	Shaded	Shaded	0,17127	5,5799	0,005	**
t0	t3			0,09391	2,7985	0,01	*
t1	t3			0,01967	0,5217	0,036	*
t0	t1	Cooled	Cooled	0,06927	2,0094	0,235	
t0	t3			0,02812	0,7811	0,573	
t1	t3			0,05665	1,5614	0,069	

Supplementary Methods

AHS computation

Treatment-specific heat exposure trajectories were quantified using Accumulated Heat Stress (AHS; an *in-situ* DHW equivalent), computed from daily *in-situ* mean temperatures relative to an *in-situ*-corrected maximum monthly mean (MMM).

Baseline MMM value was obtained from satellite-derived NOAA climatologies (MMM_{NOAA}; NOAA Coral Reef Watch Program using GPS coordinates of our study site; Liu et al. 2017). This value was then corrected to reflect local *in-situ* thermal conditions using the mean offset between daily satellite sea surface temperature (SST) and daily *in-situ* temperatures derived from multi-year logger records (2022-2025), following the approach of Claar et al. (2019). Offsets were computed using *in-situ* timeseries from our study site at 13m (~depth of coral collection). For each experiment, a linear regression between satellite SST and corresponding *in-situ* daily means was fitted. Statistically significant coefficients (slope and intercept; $R^2 > 0.95$) were then used to correct MMM_{NOAA}. The resulting *in-situ*-corrected MMM was 28.67°C.

Two AHS metrics were subsequently computed as rolling 12-week sums of positive weekly anomalies above the corrected MMM: $AHS_{0°C}$ (threshold MMM+0°C) capturing low-magnitude heat stress, and $AHS_{1°C}$ (threshold MMM+1°C) capturing moderate-to-severe stress (Kim et al. 2019; Lachs et al. 2021). AHS trajectories were calculated separately for each nursery (control & shaded vs cooled) using the corresponding *in-situ* logger time series over the 2024 MHW.

Color score quantification

We quantified pigmentation dynamics of coral fragments using a standardized RGB-based color score, providing a non-invasive and objective proxy of symbiosis status, following the approach described in Hackerott et al. (2025). At each main survey (t_0-t_3), fragments were photographed outdoors under the shade, on a white background next to a Keldan color checker card, using an Olympus TG-7 camera at a fixed distance. For each fragment, two photographs (front and back) of the flattest surface were taken to maximize visible coral area while minimizing harsh shadows.

For each image, mean color intensities were extracted for the red, green and blue channels (RGB) from three large rectangles of visible tissue, avoiding inner-branch shadows. Mean RGB values were then standardized by dividing each channel by the corresponding reference channel extracted from the color checker card, correcting for variation in ambient lighting among photographs. The resulting standardized RGB triplets were used to characterize the color profile of each fragment.

Euclidean distance matrices of standardized RGB values were computed and subjected to principal component analysis (PCA; *prcomp* function), allowing dimensionality reduction of the color space. Coordinates along the first principal axis (PC1) were extracted and used as a continuous color score, representing a gradient of color loss or gain associated with symbiont depletion or acclimation (Hackerott et al. 2025). For modelling convenience, the color score was shifted by adding a constant equal to the absolute value of the minimum score, ensuring positive values across the dataset.

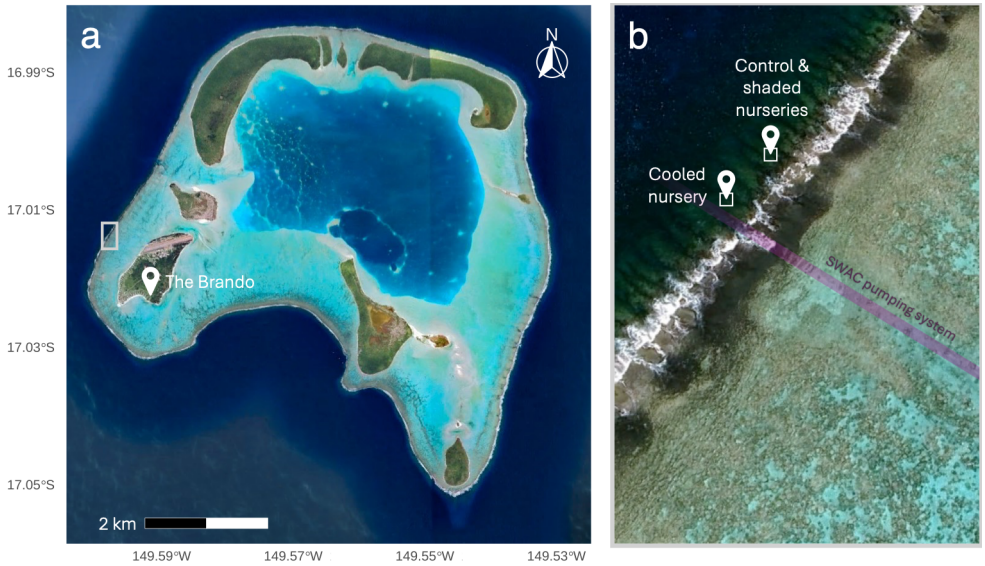

Supplementary Figure 16. Map of the study site in Tetiaroa atoll, French Polynesia. (a) The study site was located on the southern-western outer reef slope, because of the existing outlet of the (b) sea water air conditioning system (SWAC), pumping deep cold-water (960m, 11°C), operated by the resort The Brando on the adjacent islet. After being used to cool onshore infrastructures, water is rejected, unaltered, onto the reef at 30m, averaging 11°C. (b) The cooled nursery was hence installed close to the water outlet, and control and shaded nurseries were installed ~90m north-east to avoid contamination from cold-water.

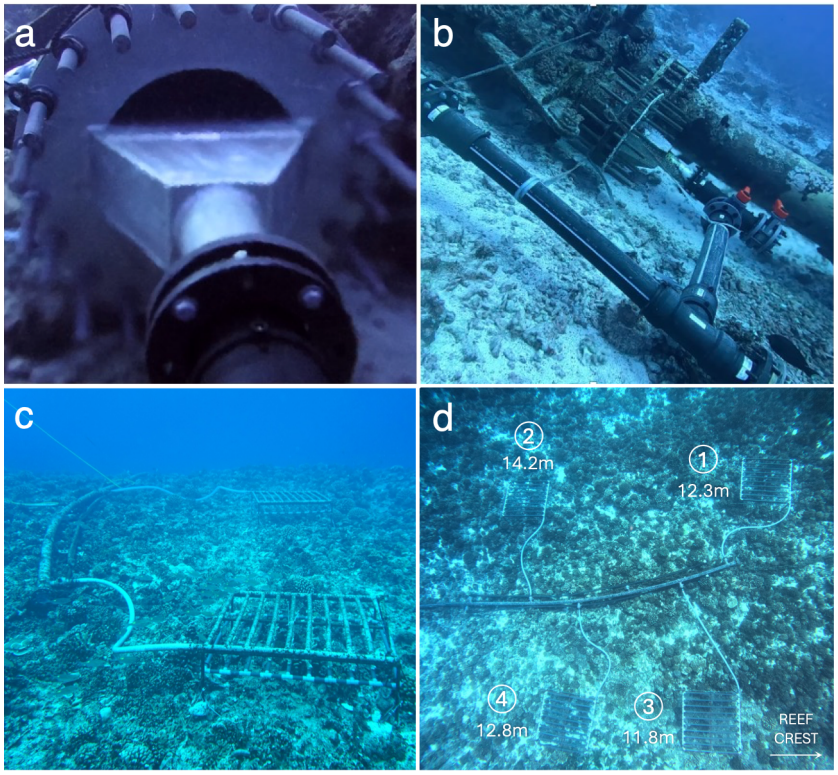

Supplementary Figure 17. Deep cold-water diffusion system used to cool coral nurseries. (a) A derivation nozzle directly connected to the SWAC outlet at 30m depth allows the recovery of ~80% of the discharged cold water. (b) Owing to the high flow rate (150-200 m^3 h^{-1}), cold water is transported under pressure upward to 12-14m depth through PVC pipes. (c) Cold water is then distributed through perforated PVC diffusion frames to cool the area directly beneath the structure. (d) The two nursery tables used in this study correspond to tables 1 and 2.

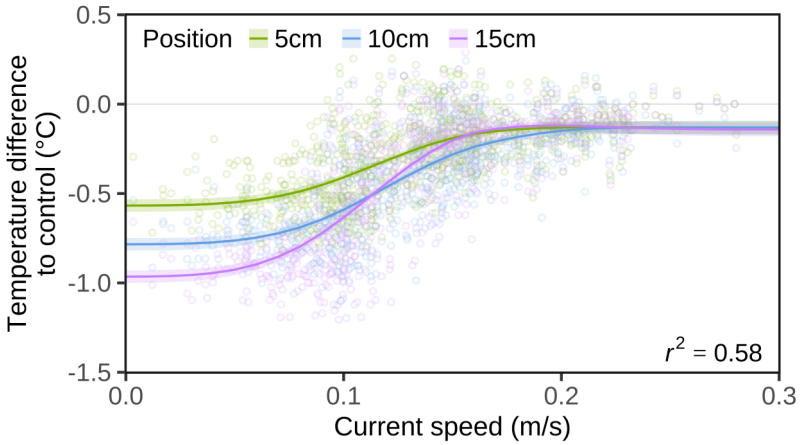

Supplementary Figure 18. Cooling capacity of the deep cold-water diffusion system. Three temperature loggers (HOBO Pro v2) were vertically deployed at the center of a table for one week (11-19 September 2023), with sensors positioned at 5, 10 and 15cm below the diffusion system. Temperature was recorded every 15minutes at these three positions and at the control site (12-13m depth), while current speed was concurrently measured using a Marotte HS current meter. Because cold water is denser, cooling intensity increased with depth below the diffusion system and was strongest at 15cm during calm hydrodynamic conditions (-0.8 to -1°C when < 0.08m/s). Based on the average height of fragments, PVC frames supporting fragments were therefore installed 20cm below the diffusion system, positioning fragments at ~15cm below the outlet to maximise cooling efficiency.

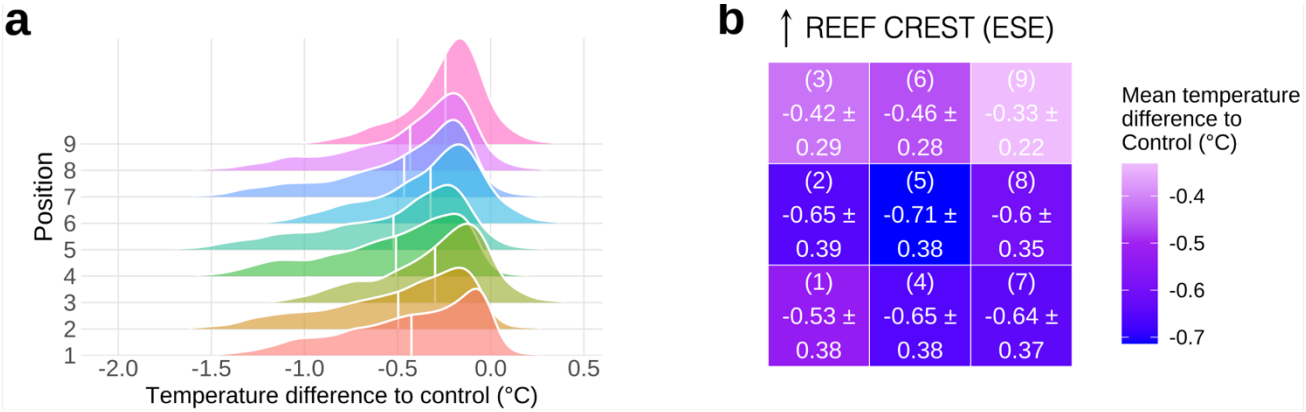

Supplementary Figure 19. Horizontal diffusion of deep cold-water plume within a coral nursery table. Nine HOBO Pro v2 temperature loggers were deployed across cooled table 1 from 1 to 23 June 2024, positioned at fragment height (15 cm from the diffuser outlet). (a) Density plots of temperature at each position; white horizontal bars indicate mean values. (b) Spatial arrangement of logger positions relative to reef crest orientation, with corresponding mean ± sd temperatures. Within-table temperature heterogeneity reflects slight reef-topography-induced tilting of the structure. Positions 3, 6 and 9 were located marginally higher, limiting cold-water retention. Because deep seawater is denser, it preferentially diffused downward and along prevailing currents, resulting in reduced cooling efficiency along the east-south-east sector of the table (~parallel to the reef crest) during this period.

Supplementary Table 5. Number of fragments snap frozen in April (t_1) and November (t_3). Genotype 33 was not snap-frozen in April (t_1) under the control treatment because one of the three fragments was lost; the remaining fragment was therefore preserved for snap-freezing in November (t_3).

	Acropora globiceps		***Pocillopora cf. tuahiniensis***		***Pavona duerdeni***	
	April	*November*	*April*	*November*	*April*	*November*
Control	15	14	15	7	14	9
Shaded	15	15	15	11	15	15
Cooled	15	15	15	5	15	10

Supplementary Table 6. Summary of all final models fitted. Explained variability is expressed through marginal R^2 (R^2_m, variability explained by the fixed effects) and conditional R^2 (R^2_c, variability explained by both fixed and random effects) when random effects were retained

	Model chosen	**Family distribution**	**Explained variability**
Temperature *daily means*	Mean ~ Treatment + (1|Date) *filtered for data during treatment*	Gaussian	R^2_m = 11%; R^2_c = 93%
daily range	Range ~ Treatment + (1|Date) *filtered for data during treatment*	Gaussian	R^2_m = 19%; R^2_c = 40%
current speed	Temperature difference to control ~ s(Current speed, bs = "cr", k = 6) + s(Date, bs = "re")	Gaussian	R^2 = 68%
Nutrients *All*	Concentration ~ Treatment*Nutrient	Gamma log link	R^2 = 96%
dissolved inorganic nitrogen (DIN)	Concentration ~ Treatment + (1|Sampling date)	Gamma log link	R^2_m = 77%; R^2_c = 83%
pH	pH ~ Treatment + (1|DateTime) + (1|Date) + (1|Time)	Gaussian	R^2_m = 5%; R^2_c = 96%
	pH ~ Temperature difference to control + (1|Date) + (1|Time)	Gaussian	R^2_m = 12%; R^2_c = 63%
Dissolved oxygen	DO ~ Treatment + (1|DateTime) + (1|Date) + (1|Time)	Gaussian	R^2_m = 1%; R^2_c = 96%
Light *daily light integral*	Friedman rank-sum tests (assumption of normality not met) followed by Wilcoxon pairwise post-hoc tests		
Bleaching probability	Bleaching[1 if bleached; 0 if not] ~ Treatment*Species *Acropora globiceps not included ; only control and shaded fragments*	Binomial	R^2 = 13%
Survival	Status_final ~ Treatment*Species	Multinomial	R^2 = 35%
Growth rate	Growth ~ Treatment*Period*Species +(1|Genotype)	Gamma log link	R^2_m = 62%; R^2_c = 75%
Photo-physiology *color score*	Color score ~ Treatment*Timepoint*Species+ +(1|Genotype)	Gamma log link	R^2_m = 72%; R^2_c = 76%
symbiont density	sqrt(10^5 cells/cm^2) ~ Treatment*Species*Timepoint + (1|Genotype/Tube)	Gaussian	R^2_m = 64%; R^2_c = 98%
chlorophyll a per symbiont	log(Chl a/symbiont) ~ Treatment*Species*Timepoint + (1|Genotype/Tube)	Gaussian	R^2_m = 47%; R^2_c = 70%
chlorophyll c2 per symbiont	log(Chl c2/symbiont) ~ Treatment*Species*Timepoint + (1|Genotype/Tube)	Gaussian	R^2_m = 39%; R^2_c = 63%

Energy stores *proteins*	log(Proteins/cm^2) ~ Treatment*Species*Timepoint + (1|Genotype/Tube)	Gaussian	R^2_m = 29%; R^2_c = 99%
lipids	log(Lipids/cm^2) ~ Treatment*Species*Timepoint + (1|Genotype/Tube)	Gaussian	R^2_m = 31%; R^2_c = 89%
carbohydrates	log(Carbohydrates/cm^2) ~ Treatment*Species*Timepoint + (1|Genotype/Tube)	Gaussian	R^2_m = 60%; R^2_c = 97%
total energy stores	log(Total energy/cm^2) ~ Treatment*Species*Timepoint + (1|Genotype)	Gaussian	R^2_m = 43%; R^2_c = 58%